Langmuir

Article

pubs.acs.org/Langmuir

Hierarchical Hydrodynamic Flow Confinement: Efficient Use and Retrieval of Chemicals for Microscale Chemistry on Surfaces

Julien Autebert, Aditya Kashyap, Robert D. Lovchik, Emmanuel Delamarche, and Govind V. Kaigala*

IBM Research−Zürich, Säumerstrasse 4, CH-8803 Rüschlikon, Switzerland

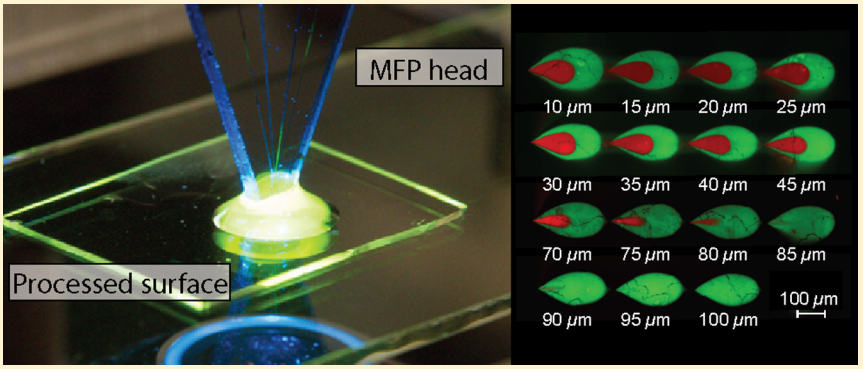

ABSTRACT: We devised, implemented, and tested a new concept for efficient local surface chemistry that we call hierarchical hydrodynamic flow confinement (hierarchical HFC). This concept leverages the hydrodynamic shaping of multiple layers of liquid to address challenges inherent to microscale surface chemistry, such as minimal dilution, economical consumption of reagent, and fast liquid switching. We illustrate two modes of hierarchical HFC, nested and pinched, by locally denaturing and recovering a 26 bp DNA with as little as 2% dilution and by efficiently patterning an antibody on a surface, with a 5 μm resolution and a 100-fold decrease of reagent consumption compared to microcontact printing. In addition, valveless switching between nanoliter volumes of liquids was achieved within 20 ms. We believe hierarchical HFC will have broad utility for chemistry on surfaces at the microscale.

1. INTRODUCTION

Many techniques have been successfully developed for patterning surfaces on the micrometer length scale and with chemistries suited for applications in microtechnology, bioanalytical sciences, and medical diagnostics. These techniques involve lithography, soft lithography, and its numerous variants,[1] as well as the accurate dispensing of (bio)chemicals using spotters[2] and inkjet printers.[3] Many of these techniques have been combined with self-assembly,[4] macromolecular systems,[5] and templated substrates[6] to achieve precise, complex, and robust chemistry on surfaces.

A specific set of techniques operating in liquid environments, which are often critical for biological systems, have been developed for processing surfaces and probing biological interfaces in the "open space".[7] These techniques operate at micrometer and submicrometer length scales and are based on scanning probe microscopy methods,[8−13] microelectrochemistry,[14−19] multiphase systems,[20−23] and hydrodynamic flow confinement (HFC) of liquids.[24−36] HFC generated using a microfluidic probe (MFP) is of particular interest because it can localize liquids on surfaces independently of the chemical composition of the confined liquids and without the need for electromigration of charged species.[29,30] Using MFPs, we, as well as other groups, showed how to pattern arrays of proteins,[29] detach single adherent cells from a surface,[29] stain living cells,[30] locally perfuse brain slices,[33] perform pharmacological studies on single cells,[25] and produce arbitrary chemical gradients on surfaces.[29,31]

While HFC proved to be well-suited for performing a range of chemical reactions on surfaces, shaping liquids over surfaces using HFC is still in its infancy. To exploit the opportunities of HFC fully, it would be strategic to redefine the methods for bringing/removing chemicals onto/from a surface. Here we describe a new concept, called hierarchical HFC, wherein multiple layers of liquids are shaped to get into contact with a surface. We illustrate how hierarchical HFC can readily address critical aspects of microscale surface chemistry through minimal dilution of chemicals in a spatially defined region of a surface, efficient retrieval of chemicals, and fast and simple switching between confined liquids.

2. MATERIAL AND METHODS

2. 1. Numerical Simulations. For numerical simulations, we made use of laminar flows and diffusion modules of COMSOL Multiphysics (COMSOL, MA) and constructed a model that considers incompressible fluids, open boundaries, and nonslip conditions on surfaces. The model couples the solution of Navier−Stokes equation and the convection−diffusion equation. Both the processing liquid and the

Received: March 6, 2014
Published: March 13, 2014

   dx.doi.org/10.1021/la500875m | *Langmuir* 2014, 30, 3640−3645

immersion liquids were chosen to be water (incompressible Newtonian fluid with a density of 998 kg m^{-3} and dynamic viscosity of 0.001 N s m^{-2}), while all the boundaries of the head liquid outside of the injection/aspiration channels were defined as open (at atmospheric pressure). A nonslip condition was defined on the surface of the substrate and of the MFP head, and simulations were run in steady state. Additional rules for flow rates were empirically chosen as injection and aspiration through the two inner apertures set to be equal ($Q_{i2} = Q_{a1}$) to ensure minimal dilution, and the total aspiration was set to be 3× the total injection [$Q_{a1} + Q_{a2} = 3(Q_{i1} + Q_{i2})$] to ensure a stable outer HFC.

2.2. MFP Head Design, Microfabrication, and MFP Platform. The MFP consists of a microfabricated head mounted on a platform placed on top of an inverted microscope. The microfabrication of the head and the MFP platform have previously been described.[30] Briefly, the head was designed using L-Edit (Tanner EDA), and a chromium mask was written using a laser writer (WL 2000, Heidelberg Instruments Mikrotechnik GmbH). A 400 μm thick Si layer was etched using deep reactive ion etching (DRIE) and anodically bonded to a 500 μm thick glass wafer. After bonding, the 4 channels (50 × 50 μm^2 section, spacing between apertures = 50 μm) were filled with wax and the bonded silicon/glass wafers were diced to form individual heads, which were polished. The heads were cleaned and used with an MFP platform[37] that sits on an inverted microscope (Nikon Eclipse). Images were acquired using an ORCA-Flash 4.0 camera (Hamamatsu) and a LED lamp (Sola, Lumencore).

2.3. MFP Head Apex-to-Surface Distance Control and Tilt Adjustment. The apex-to-surface distance (d) is monitored using the position of the stage that is encoded. Prior to the use of the MFP, we establish the zero position by approaching the surface with the apex until Newton rings form between the glass slide and the apex of the MFP, using a computer-controlled motorized linear stage (Lang GmbH, Huettenberg, Germany). This defines the zero position of the head in the z direction. While in this "contact mode," the tilt of the apex is corrected by centering the Newton rings in the middle of the apex. This process is repeated on five positions to adjust the planarity of the entire glass slide (25 × 75 mm), and the holder is adjusted accordingly. With five control positions on the glass surface, we observed a tilt of the processed surface below 1 μm per cm, resulting in a tilt of the apex below 0.1°. Precision on the z position is defined by the linear stage, which is below 0.5 μm with a linearity deviation of 1 μm over the range of 100 mm. Since the MFP operates in a noncontact mode, minor variations of the apex-to-surfaces do not impact surface processing, allowing for efficient scanning and processing of large areas.

2.4. Flow Control and Spectrophotometry. All flows were controlled using computer-controlled syringe pumps (Cetoni GmbH) and 50 μL glass syringes (Hamilton, Bonaduz, Switzerland). A flow-through spectrophotometer (Cetoni GmbH, Korbussen, Germany) was used to measure the concentration of the food dye in the aspirated liquid. Prior to concentration measurements, a normalizing solution is passed through the spectrophotometer and the absorbance is measured. This value, along with a blank measurement with DI was used to calibrate the spectrophotometer to estimate the concentration of the dye as a fraction of the control solution.

2.5. Printing and Removal of Antibodies and Oligonucleotides. We used microcontact printing to pattern 500 × 500 μm^2 squares of antibiotin antibodies (Sigma-Aldrich, St Louis, MO) on a plasma-treated glass surface.[38] We then bound a 26 bp double stranded (ds) DNA comprising a biotin on the 5′ end of the first oligonucleotide (Biotin/TGG GCG GCA TGA ACC GGA GGC CCA TC, Integrated DNA Technologies, Coralville, IA) and a fluorescent dye at the 5′ end of the second oligonucleotide (AlexaFluor 546/GAT GGG CCT CCG GTT CAT GCC GCC CA) to the printed antibodies. Removal of the second strand of the DNA was achieved by denaturing the hydrogen bond using a 0.5 M NaOH solution.

Deposition of antibodies (goat antimouse IgG, Invitrogen, Carlsbad, CA) labeled with a green fluorophore (AlexaFluor 488) or a red fluorophore (AlexaFluor 555) on an NHS-activated glass slide (HC polycarboxylate hydrogel, NHS-activated, XanTec Bioanalytics GmbH, Germany) was achieved by rehydrating the glass slide 5 min in DI prior to each experiment.

3. RESULTS AND DISCUSSION

3.1. Hierarchical Flows. Creating a HFC using a MFP relies on (1) bringing two coplanar apertures in proximity to a surface in (2) the presence of an immersion liquid, and (3) injecting a liquid from a first aperture at a flow rate Q_i that is smaller than the aspiration flow rate Q_a through the second aperture (Figure 1a). As a result, the injected liquid is confined

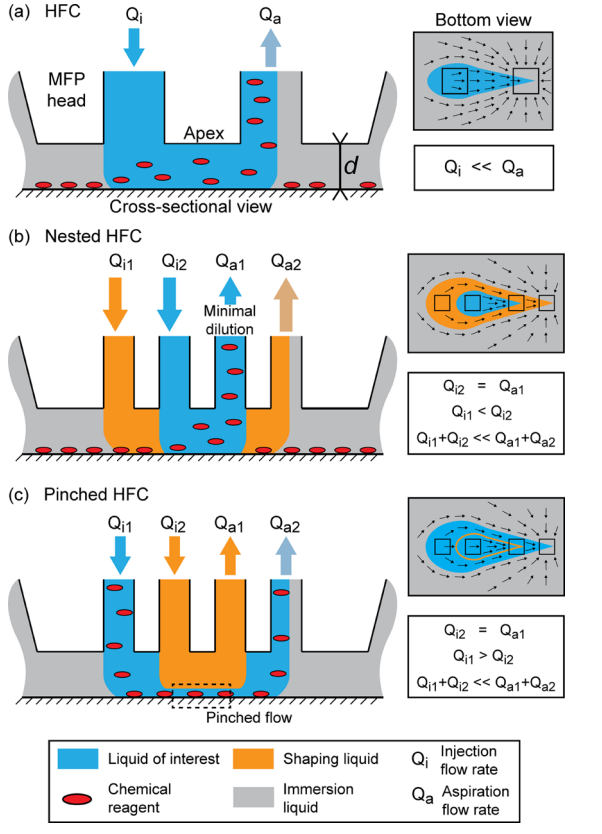

Figure 1. Principle of HFC and hierarchical HFC. (a) In the classical HFC, a processing liquid (blue) is confined, in the presence of an immersion liquid, between the apex of the MFP head and the surface. The addition of a shaping liquid (orange) and setting the injection and aspiration flow rates of the liquids appropriately enable (b) nested HFC or (c) pinched HFC for efficient use or recovery of chemicals during local surface processing.

dx.doi.org/10.1021/la500875m | Langmuir 2014, 30, 3640−3645

hydrodynamically between the apex of the MFP head and the surface to be processed, with an apex-to-surface distance d. This liquid can contain critical ligands for analytes on a surface or can be used to detach and retrieve different compounds from a surface.[29,30]

In previous work,[30] a stable and well-defined flow confinement was achieved for processing surfaces using $Q_a = 3Q_i$. A significant drawback of this asymmetry in the flow rates is the dilution of the liquid of interest by the immersion liquid. In a first example of hierarchical HFC, we use two extra apertures to "nest" a liquid of interest inside another shaping liquid that is itself confined within the immersion liquid (Figure 1b). Therefore, the relation between the injection and aspiration flow rates can be distributed unequally between the nested liquid and the intermediate (shaping) liquid without affecting the stability of the flow confinements. In addition, dilution of chemical species retrieved from the surface can be minimized in the nested liquid. Another strategy, named "pinched HFC", is realized by adjusting the ratio of flow rates ($Q_{i1}/Q_{i2} > 1$, Figure 1c). In this case, the liquid of interest is pinched against the surface using the shaping liquid. This strategy relates to what has been demonstrated using hydrodynamic flow focusing in FACS[39] or pinched-flow fractionation devices,[40−43] where one or multiple laminar flows are used to shape a critical liquid. Pinched HFC enables a dramatic reduction in the consumption of reagents for microscale chemistry on surfaces by excluding a volume between the MFP head and the surface that is not critical.

3.2. Numerical Simulations Results. We used finite element modeling to gain insight into hierarchical HFC and relevant operating conditions. For a given ratio Q_{i1}/Q_{i2}, the distance d between the apex of the MFP head and the surface defines which of the HFC modes operates (Figure 2). In nested HFC, d can of course be varied to adjust the footprint of the processing liquid on the surface. Increasing d leads to switching to pinched HFC. During the transition from nested to pinched HFC, molecules in the processing liquid may still reach the surface by diffusion through the pinched liquid (see diffusion zone in Figure 2). This diffusion zone was calculated for an IgG molecule ($D = 4 \times 10^{-7}$ cm^2 s^{-1}).[44] A strong advantage of pinched HFC is of course the reduction of reagent consumption for processing a surface. This reduction is ultimately limited by the lateral displacement of the processing liquid under strong pinching conditions. Using larger inner apertures can limit this expansion and can widen operable flow conditions for pinched HFC. Interestingly, switching between nested and pinched HFCs can be achieved by simply modifying the ratio Q_{i1}/Q_{i2} or by changing d. Perturbation to the shape of HFCs may occur when the apex of the MFP head and the surface are not parallel. The apex of the head can be tilted parallel or perpendicular to the flow of the processing liquid at the apex. In the scenario of a tilt parallel to the flow, the distance to surface varies for each aperture, yet symmetry is conserved and the shape of the HFCs will remain unchanged, with an increased flow velocity in the vicinity of the aperture closer to the surface. In the scenario that the tilt of the head is perpendicular to the flow, the symmetry is modified and hydraulic resistance increases in the section of the apex closer to the surface, leading to a lateral displacement of the HFCs. However, we found that the tilt measured after parallelism adjustment is below 0.1°, or a difference between the two edges below 1 μm. In practice, this tilt is very small, we therefore did not investigate the effect of high tilt angles on the HFC.

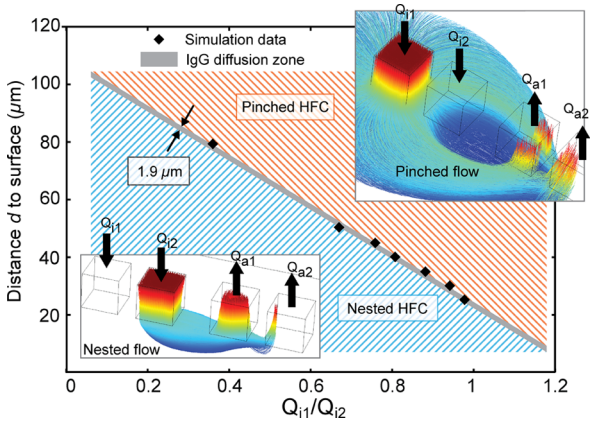

Figure 2. Numerical simulations showing the effect of the injection ratio Q_{i1}/Q_{i2} on the minimal distance between the MFP head and the surface for which the inner (nested) liquid loses contact with the surface. Using the diffusion characteristics of an IgG, a gray line highlights how diffusion can bring a molecule in the nested flow into contact with the surface. Both inserts are 3D particle-tracking simulations, in which the color of the paths represents the particle-to-surface distance (dark blue for $d = 0$ and red for $d = 100$ μm).

3.3. Investigating Minimal Dilution. On the basis of this understanding of the operating conditions of hierarchical HFC, we microfabricated a MFP head to investigate the dilution of a sample in the inner HFC. Specifically, we used a nested liquid containing a food dye and measured its concentration in the inner aspiration channel.

Figure 3 presents the concentration of the dye (C_m) measured in the inner aspiration aperture normalized with the injected concentration C_i for different flow ratios Q_{i2}/Q_{a1}. The outer injection and aspiration flow rates were set to $Q_{a1} + Q_{a2} = 3(Q_{i1} + Q_{i2})$ to ensure a stable HFC of the shaping and nested liquids. A ratio of $C_m/C_i < 1$ corresponds to a dilution of the dye by some of the liquid used for creating the HFC

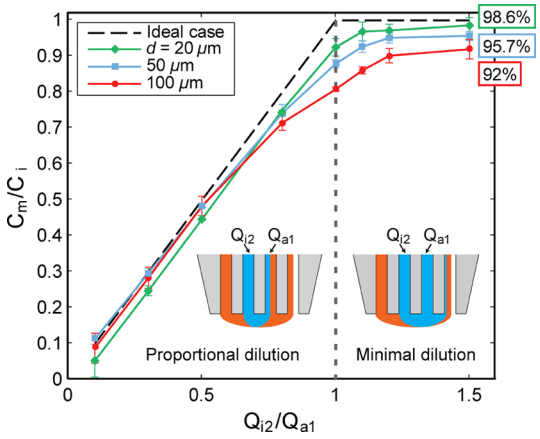

Figure 3. Dilution of a dye (initial concentration C_i and concentration in the aspiration aperture C_m) in a nested liquid as a function of Q_{i2}/Q_{a1} for various apex-to-surface distances (d = 20, 50, and 100 μm). Here, Q_{i1} and Q_{a2} are fixed, and the diffusion at the boundary between both HFCs is neglected for the ideal case. Error bars represent standard deviation ($n = 3$). The drawings illustrate the distribution of the nested liquid (blue) between the apertures. Shaping liquid is shown in orange, immersion liquid and processed surface are omitted for clarity.

dx.doi.org/10.1021/la500875m | Langmuir 2014, 30, 3640−3645

condition. This dilution is directly proportional to Q_{i2}/Q_{a1} as long as the injection flow rate Q_{i2} remains smaller than the aspiration flow rate Q_{a1}. In this proportional dilution regime, the confinement of the inner liquid does not take advantage of hierarchical HFC and behaves similarly to a "classical" HFC. However, when the injection flow rate Q_{i2} is higher than the aspiration flow rate Q_{a1}, we observed that most of the liquid entering the inner aspiration aperture comes from the inner injection aperture. In this case, dilution of the dye is very small, and C_m converges toward C_i. This regime, which we call "minimal dilution" is increasingly more efficient in preventing dilution of the dye as the apex-to-surface distance d reduces. The shaping liquid helps create a stable HFC for the inner liquid without the need for a strong asymmetry of aspiration and injection as used in classical HFC. Taking the example of d = 20 μm, the nested liquid experienced a dilution of less than 2%, whereas the dilution of an injected liquid in classical HFC is typically 3-fold ($Q_a = 3Q_i$). We hypothesize that diffusion of the dye out of the nested liquid accounts for the small dilution (1.4 to 8%) observed in Figure 3. This is consistent with the observation that dilution decreases with d: the envelope of the nested liquid flattens and increases its contact area with the surface at smaller d, thereby reducing the total diffusion area between the nested and shaping liquids. Nested HFC not only minimizes dilution of chemicals in a liquid of interest but can also be used for efficient retrieval of reagents/analytes from a surface.

3.4. Surface Processing Using Hierarchical HFC. We illustrate how hierarchical HFC can be used for microscale chemistry on surfaces by providing a few examples below. First, we removed functionalized DNA from a surface (Figure 4, panels a and b). After deposition using microcontact printing, we injected a solution of NaOH (0.5 M)[45] using the inner HFC in the nested mode to denature DNA locally and remove the fluorescently labeled DNA strand from the surface (Figure 4, panels a and b). This was done by positioning the MFP head at d = 20 μm with an injection-to-aspiration ratio of 1.2 (flow rates: Q_{i1} = 0.8 μL min^{-1}, Q_{i2} = 1.2 μL min^{-1}, Q_{a1} = 1 μL min^{-1}, Q_{a2} = 5 μL min^{-1}). This resulted in a dilution of the denaturation solution with the immersion liquid of ~2% (Figure 3). We calculated a 6-fold increase in the concentration of the DNA retrieved from the surface using the nested-HFC compared to classical HFC with the same flow rates. The local denaturation of the ds DNA resulted in 90% removal of the fluorescently labeled DNA and was reversible: incubating the processed surface with the fluorescently labeled single-stranded DNA led to a recovery of fluorescence (data not shown). This example of processing a surface and minimizing dilution during retrieval of a chemical from a surface might be important for surface analysis and for recovering precious samples, such as nucleic acids or other ligands, from specific sites on microarrays or from selected adherent cells, for example.

Another demonstration of hierarchical HFC is the simultaneous deposition of two proteins on a surface using compartmentalization of the proteins in either the inner or the outer HFC. This was done by depositing antibodies labeled with a green or red fluorophore on an NHS-activated glass slide (Figure 4, c and d). Here, flow rates were kept constant (Q_{i1} = 1 μL min^{-1}, Q_{i2} = 1 μL min^{-1}, Q_{a1} = 1 μL min^{-1}, and Q_{a2} = 5 μL min^{-1}) but d was varied so as to select the footprint of the inner antibody pattern (shown in red) on the functionalized glass slide. For these flow conditions and aperture geometries, d = 85 μm was the critical distance at which the inner liquid

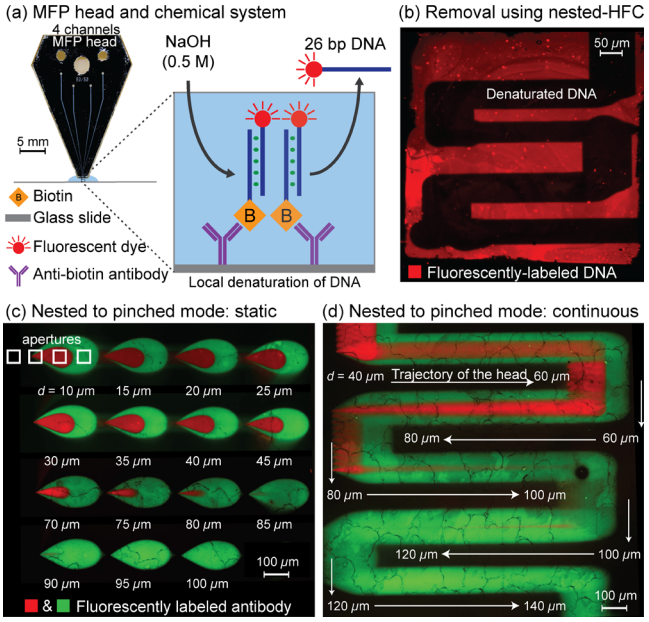

Figure 4. Microscale removal and deposition of chemical species from/onto a glass surface. (a) Image of a MFP head having 4 channels and apertures for hierarchical HFC (left) and sketch of the chemical system (right) used for (b) local denaturation of DNA on a surface. (c) Assembly of fluorescence images showing the simultaneous patterning of antibodies on a surface using hierarchical HFC (red-labeled antibodies are in the nested liquid and green-labeled antibodies in the shaping liquid). The deposited patterns of antibodies reflect the transition from nested to pinched HFC mode at increasing d. (d) Patterning of the same antibodies as in (c), with d continuously varied (+1 μm s^{-1}) during scanning (x/y speed of MFP head of 50 μm s^{-1}).

stopped being nested and became lifted as in the pinched HFC configuration. Continuous patterning can also be done by varying d during motion of the MFP head over the surface (Figure 4d). This can be a simple method for creating complex gradients of chemicals on a surface. Moreover, switching from a nested to a pinched HFC mode enables efficient and fast switching between different processing conditions by simply changing d instead of switching between liquids using valves. We readily achieved a switching time of ~20 ms by varying d from 10 to 100 μm (Figure 4c). This approach might be used for briefly stimulating cells with chemicals or retrieving factors excreted by cells.[46]

Interestingly, the resolution of patterns created on surfaces can be increased by modulating the distance d as shown in Figure 4 (panels c and d). We also calculated a 3-fold decrease in the consumption of chemical reagents when processing a surface using the outer flow in pinched HFC mode compared to classical HFC. As an example, writing a 100 × 100 μm^2 pattern of antibody only needs 16.7 nL of antibody solution using pinched HFC (1 s writing time at 1 μL min^{-1} flow rate) compared to ~50 nL without pinching the antibody solution and one to a few microliters using microcontact printing.[47]

Key parameters in the establishment and control of the hierarchical HFCs are injection and aspiration flow rates and distance d. The precision in measuring d (±1 μm) is higher than, for example, the diffusion length for an IgG molecule; we therefore can reliably process large areas of surface without any modification to the hierarchy of flows. In addition, the HFC quickly adapts to irregular surface topography, for example, over adherent cells and tissue sections.[36]

dx.doi.org/10.1021/la500875m | Langmuir 2014, 30, 3640−3645

4. CONCLUDING REMARKS

We believe that hierarchical HFC holds great promise for efficient microscale chemical processing of surfaces because it neither requires working with particular liquids nor depends on experimentally challenging conditions. This concept is therefore broadly applicable and well-suited for working with biological interfaces. In addition, the outer liquid can be used for protecting the inner apertures or a surface from clogging by particulates or toxic chemicals, respectively. We hypothesize that shielding the inner apertures from particles and shaping the nested HFC could lead to submicrometer surface processing using the MFP. Hierarchical HFC can also solve the challenge of working with an immersion liquid and a processing liquid that are nonmiscible by inserting a liquid having an intermediate surface tension. Overall, hierarchical HFC is simple, flexible, interactive, and should greatly enhance methods based on HFC for shaping liquids over surfaces.

AUTHOR INFORMATION

Corresponding Author

*E-mail: gov@zurich.ibm.com.

Notes

The authors declare no competing financial interest.

ACKNOWLEDGMENTS

We are grateful to Martina Hitzbleck and Julien Cors for discussions. We thank Marcy Zenobi-Wong (ETHZ), Urs Dürig, and Walter Riess for their continuous support. We acknowledge financial support by the European Research Council (ERC) Starting Grant, under the 7th Framework Program (Project 311122, "BioProbe").

ABBREVIATIONS

HFC, hydrodynamic flow confinement; MFP, microfluidic probe; FACS, fluorescence-activated cell sorting; IgG, immunoglobulin G

REFERENCES

(1) Xia, Y.; Whitesides, G. M. Soft Lithography. *Angew. Chem., Int. Ed.* **1998**, *37*, 550−575.
(2) MacBeath, G.; Schreiber, S. L. Printing Proteins as Microarrays for High-Throughput Function Determination. *Science* **2000**, *289*, 1760−1763.
(3) Delaney, J. T.; Smith, P. J.; Schubert, U. S. Inkjet Printing of Proteins. *Soft Matter* **2009**, *5*, 4866.
(4) Lee, I. Molecular Self-Assembly: Smart Design of Surface and Interface via Secondary Molecular Interactions. *Langmuir* **2013**, *29*, 2476−2489.
(5) Stamou, D.; Duschl, C.; Delamarche, E.; Vogel, H. Self-Assembled Microarrays of Attoliter Molecular Vessels. *Angew. Chem., Int. Ed.* **2003**, *42*, 5580−5583.
(6) Kraus, T.; Malaquin, L.; Schmid, H.; Riess, W.; Spencer, N. D.; Wolf, H. Nanoparticle Printing with Single-Particle Resolution. *Nat. Nanotechnol.* **2007**, *2*, 570−576.
(7) Kaigala, G. V; Lovchik, R. D.; Delamarche, E. Microfluidics in the "Open Space" for Performing Localized Chemistry on Biological Interfaces. *Angew. Chem., Int. Ed.* **2012**, *51*, 11224−11240.
(8) Piner, R. D. "Dip-Pen" Nanolithography. *Science* **1999**, *283*, 661−663.
(9) Ginger, D. S.; Zhang, H.; Mirkin, C. A. The Evolution of Dip-Pen Nanolithography. *Angew. Chem., Int. Ed.* **2004**, *43*, 30−45.
(10) Kim, K.-H.; Moldovan, N.; Espinosa, H. D. A Nanofountain Probe with Sub-100 Nm Molecular Writing Resolution. *Small* **2005**, *1*, 632−635.
(11) Kim, K.-H.; Sanedrin, R. G.; Ho, A. M.; Lee, S. W.; Moldovan, N.; Mirkin, C. A.; Espinosa, H. D. Direct Delivery and Submicrometer Patterning of DNA by a Nanofountain Probe. *Adv. Mater.* **2008**, *20*, 330.
(12) Meister, A.; Gabi, M.; Behr, P.; Studer, P.; Vörös, J.; Niedermann, P.; Bitterli, J.; Polesel-Maris, J.; Liley, M.; Heinzelmann, H.; et al. FluidFM: Combining Atomic Force Microscopy and Nanofluidics in a Universal Liquid Delivery System for Single Cell Applications and Beyond. *Nano Lett.* **2009**, *9*, 2501−2507.
(13) Dörig, P.; Stiefel, P.; Behr, P.; Sarajlic, E.; Bijl, D.; Gabi, M.; Vörös, J.; Vorholt, J. a.; Zambelli, T. Force-Controlled Spatial Manipulation of Viable Mammalian Cells and Micro-Organisms by Means of FluidFM Technology. *Appl. Phys. Lett.* **2010**, *97*, 023701.
(14) Bruckbauer, A.; James, P.; Zhou, D.; Yoon, J. W.; Excell, D.; Korchev, Y.; Jones, R.; Klenerman, D. Nanopipette Delivery of Individual Molecules to Cellular Compartments for Single-Molecule Fluorescence Tracking. *Biophys. J.* **2007**, *93*, 3120−3131.
(15) Bruckbauer, A.; Ying, L.; Rothery, A. M.; Zhou, D.; Shevchuk, A. I.; Abell, C.; Korchev, Y. E.; Klenerman, D. Writing with DNA and Protein Using a Nanopipet for Controlled Delivery. *J. Am. Chem. Soc.* **2002**, *124*, 8810−8811.
(16) Novak, P.; Li, C.; Shevchuk, A. I.; Stepanyan, R.; Caldwell, M.; Hughes, S.; Smart, T. G.; Gorelik, J.; Ostanin, V. P.; Lab, M. J.; et al. Nanoscale Live-Cell Imaging Using Hopping Probe Ion Conductance Microscopy. *Nat. Methods* **2009**, *6*, 279−281.
(17) Korchev, Y. E.; Negulyaev, Y. A.; Edwards, C. R.; Vodyanoy, I.; Lab, M. J. Functional Localization of Single Active Ion Channels on the Surface of a Living Cell. *Nat. Cell Biol.* **2000**, *2*, 616−619.
(18) Descamps, E.; Leïchlé, T.; Corso, B.; Laurent, S.; Mailley, P.; Nicu, L.; Livache, T.; Bergaud, C. Fabrication of Oligonucleotide Chips by Using Parallel Cantilever-Based Electrochemical Deposition in Picoliter Volumes. *Adv. Mater.* **2007**, *19*, 1816−1821.
(19) Momotenko, D.; Cortes-Salazar, F.; Lesch, A.; Wittstock, G.; Girault, H. H. Microfluidic Push-Pull Probe for Scanning Electrochemical Microscopy. *Anal. Chem.* **2011**, *83*, 5275−5282.
(20) Tavana, H.; Jovic, a; Mosadegh, B.; Lee, Q. Y.; Liu, X.; Luker, K. E.; Luker, G. D.; Weiss, S. J.; Takayama, S. Nanolitre Liquid Patterning in Aqueous Environments for Spatially Defined Reagent Delivery to Mammalian Cells. *Nat. Mater.* **2009**, *8*, 736−741.
(21) Tavana, H.; Mosadegh, B.; Takayama, S. Polymeric Aqueous Biphasic Systems for Non-Contact Cell Printing on Cells: Engineering Heterocellular Embryonic Stem Cell Niches. *Adv. Mater.* **2010**, *22*, 2628−2631.
(22) Tavana, H.; Mosadegh, B.; Zamankhan, P.; Grotberg, J. B.; Takayama, S. Microprinted Feeder Cells Guide Embryonic Stem Cell Fate. *Biotechnol. Bioeng.* **2011**, DOI: 10.1002/bit.23190.
(23) Yaguchi, T.; Lee, S.; Choi, W. S.; Kim, D.; Kim, T.; Mitchell, R. J.; Takayama, S. Micropatterning Bacterial Suspensions Using Aqueous Two Phase Systems. *Analyst* **2010**, *135*, 2848−2852.
(24) Smith, K. A.; Gale, B. K.; Conboy, J. C. Micropatterned Fluid Lipid Bilayer Arrays Created Using a Continuous Flow Microspotter. *Anal. Chem.* **2008**, *80*, 7980−7987.
(25) Ainla, A.; Jansson, E. T.; Stepanyants, N.; Orwar, O.; Jesorka, A. A Microfluidic Pipette for Single-Cell Pharmacology. *Anal. Chem.* **2010**, *82*, 4529−4536.
(26) Corgier, B. P.; Juncker, D. Polymeric Microfabricated Electrochemical Nanoprobe with Addressable Electrodes. *Sens., Actuators B* **2011**, *157*, 691−696.
(27) Feinerman, O.; Moses, E. A Picoliter "Fountain-Pen" Using Co-Axial Dual Pipettes. *J. Neurosci. Methods* **2003**, *127*, 75−84.
(28) Ainla, A.; Jeffries, G. D. M.; Brune, R.; Orwar, O.; Jesorka, A. A Multifunctional Pipette. *Lab Chip* **2012**, *12*, 1255−1261.
(29) Juncker, D.; Schmid, H.; Delamarche, E. Multipurpose Microfluidic Probe. *Nat. Mater.* **2005**, *4*, 622−628.
(30) Kaigala, G. V; Lovchik, R. D.; Drechsler, U.; Delamarche, E. A Vertical Microfluidic Probe. *Langmuir* **2011**, *27*, 5686−5693.

(31) Qasaimeh, M. a; Gervais, T.; Juncker, D. Microfluidic Quadrupole and Floating Concentration Gradient. *Nat. Commun.* **2011**, *2*, 464.
(32) Lovchik, R. D.; Drechsler, U.; Delamarche, E. Multilayered Microfluidic Probe Heads. *J. Micromech. Microeng.* **2009**, *19*, 115006.
(33) Queval, A.; Ghattamaneni, N. R.; Perrault, C. M.; Gill, R.; Mirzaei, M.; McKinney, R. A.; Juncker, D. Chamber and Microfluidic Probe for Microperfusion of Organotypic Brain Slices. *Lab Chip* **2010**, *10*, 326−334.
(34) Shiku, H.; Yamakawa, T.; Nashimoto, Y.; Takahashi, Y.; Torisawa, Y.-S.; Yasukawa, T.; Ito-Sasaki, T.; Yokoo, M.; Abe, H.; Kambara, H.; et al. A Microfluidic Dual Capillary Probe to Collect Messenger RNA from Adherent Cells and Spheroids. *Anal. Biochem.* **2009**, *385*, 138−142.
(35) Christ, K. V; Turner, K. T. Design of Hydrodynamically Confined Microfluidics: Controlling Flow Envelope and Pressure. *Lab Chip* **2011**, *11*, 1491−1501.
(36) Lovchik, R. D.; Kaigala, G. V; Georgiadis, M.; Delamarche, E. Micro-Immunohistochemistry Using a Microfluidic Probe. *Lab Chip* **2012**, *12*, 1040−1043.
(37) Cors, J. F.; Lovchik, R. D.; Delamarche, E.; Kaigala, G. V. A Compact and Versatile Microfluidic Probe for Local Processing of Tissue Sections and Biological Specimens. *Rev. Sci. Instrum.* **2014**, *85*.
(38) Bernard, A.; Delamarche, E.; Schmid, H.; Michel, B.; Bosshard, H. R.; Biebuyck, H. Printing Patterns of Proteins. *Langmuir* **1998**, *14*, 2225−2229.
(39) Crosland-Taylor, P. J. A Device for Counting Small Particles Suspended in a Fluid through a Tube. *Nature* **1953**, *171*, 37−38.
(40) Bhagat, A. A. S.; Hou, H. W.; Li, L. D.; Lim, C. T.; Han, J. Pinched Flow Coupled Shear-Modulated Inertial Microfluidics for High-Throughput Rare Blood Cell Separation. *Lab Chip* **2011**, *11*, 1870−1878.
(41) Lee, K. H.; Kim, S. B.; Lee, K. S.; Sung, H. J. Enhancement by Optical Force of Separation in Pinched Flow Fractionation. *Lab Chip* **2011**, *11*, 354−357.
(42) Yamada, M.; Nakashima, M.; Seki, M. Pinched Flow Fractionation: Continuous Size Separation of Particles Utilizing a Laminar Flow Profile in a Pinched Microchannel. *Anal. Chem.* **2004**, *76*, 5465−5471.
(43) Larsen, A. V.; Poulsen, L.; Birgens, H.; Dufva, M.; Kristensen, A. Pinched Flow Fractionation Devices for Detection of Single Nucleotide Polymorphisms. *Lab Chip* **2008**, *8*, 818−821.
(44) Jøssang, T.; Feder, J.; Rosenqvist, E. Photon Correlation Spectroscopy of Human IgG. *J. Protein Chem.* **1988**, *7*, 165−171.
(45) Agarwal, R. K.; Perl, A. PCR Amplification of Highly GC-Rich DNA Template after Denaturation by NaOH. *Nucleic Acids Res.* **1993**, *21*, 5283−5284.
(46) Chin, J. W.; You, L.; Kelley, S. O.; Dittrich, P. S.; Lecault, V.; White, A. K.; Singhal, A.; Hansen, C. L. Microfluidic Single Cell Analysis: From Promise to Practice. *Curr. Opin. Chem. Biol.* **2012**, *16*, 381−390.
(47) Bernard, A.; Fitzli, D.; Sonderegger, P.; Delamarche, E.; Michel, B.; Bosshard, H. R.; Biebuyck, H. Affinity Capture of Proteins from Solution and Their Dissociation by Contact Printing. *Nat. Biotechnol.* **2001**, *19*, 866−869.